

RAPID COMMUNICATION

Accuracy of combined PET/CT in image-guided interventions of liver lesions: An *ex-vivo* study

Patrick Veit, Christiane Kuehle, Thomas Beyer, Hilmar Kuehl, Andreas Bockisch, Gerald Antoch

Patrick Veit, Christiane Kuehle, Thomas Beyer, Hilmar Kuehl, Andreas Bockisch, Gerald Antoch, Department of Diagnostic and Interventional Radiology and Neuroradiology Department of Nuclear Medicine University Hospital Essen, Hufelandstrasse 55, 45122 Essen, Germany

Correspondence to: Patrick Veit, MD, Department of Diagnostic and Interventional Radiology, University Hospital of Essen, Hufelandstrasse 55, 45122 Essen, Germany. patrick.veit@uni-essen.de

Telephone: +49-201-7231528 Fax: +49-201-7231563

Received: 2005-08-26 Accepted: 2005-10-26

Key words: Liver biopsy; Radiofrequency ablation; Combined PET/CT; *ex-vivo* study; Image guided interventions

Veit P, Kuehle C, Beyer T, Kuehl H, Bockisch A, Antoch G. Accuracy of combined PET/CT in image-guided interventions of liver lesions: An *ex-vivo* study. *World J Gastroenterol* 2006; 12(15): 2388-2393

<http://www.wjgnet.com/1007-9327/12/2388.asp>

Abstract

AIM: Positioning of interventional devices in liver lesions is a challenging task if only CT is available. We investigated the potential benefit of combined PET/CT images for localization of interventional devices in interventional liver studies.

METHODS: Thirty lesions each of hyperdense, isodense and hypodense attenuation compared to normal liver parenchyma were injected into 15 *ex-vivo* pig livers. All lesions were composed of the same amounts of gelatine containing 0.5 MBq of ¹⁸F-FDG. Following lesion insertion, an interventional needle was placed in each lesion under CT-guidance solely. After that, a PET/CT study was performed. The localization of the needle within the lesion was assessed for CT alone and PET/CT and the root mean square (RMS) was calculated. Results were compared with macroscopic measurements after lesion dissection serving as the standard of reference.

RESULTS: In hypo- and isodense lesions PET/CT proved more accurate in defining the position of the interventional device when compared with CT alone. The mean RMS for CT and PET/CT differed significantly in isodense and hypodense lesions. No significant difference was found for hyperdense lesions.

CONCLUSION: Combined FDG-PET/CT imaging provides more accurate information than CT alone concerning the needle position in FDG-PET positive liver lesions. Therefore combined PET/CT might be potentially beneficial not only for localization of an interventional device, but may also be beneficial for guidance in interventional liver procedures.

© 2006 The WJG Press. All rights reserved.

INTRODUCTION

Treatment of liver lesions may be performed either surgically or interventionally. Surgery still represents the treatment of choice in solitary liver lesions or in patients with a limited number of lesions confined to a specific liver segment. However, certain cardiovascular or pulmonary risk factors may prevent patients from undergoing surgery with a curative intent^[1,2]. In some patients minimally invasive interventional approaches may serve as an option for patient treatment. Interventional procedures for treatment of liver lesions include procedures such as radiofrequency ablation, laser induced ablation or chemoembolization^[3-5]. Except for chemoembolization, all other therapeutic interventional procedures include placement of an interventional needle transcutaneously within the liver lesion. In most procedures, the needle is placed under CT, MRI, or ultrasound guidance. However, localization and guidance of an interventional device on morphological imaging can be challenging, particularly in selected cases where differentiation of the tumor from adjacent liver parenchyma may be difficult. These circumstances occur especially in tumors with only little or no contrast enhancement^[6,7]. On the other hand, functional imaging has proved to be superior to morphological imaging in detection and characterization of these tumors, but is known for only limited anatomical information.

In any case accurate placement of an interventional device is indispensable for complete tumor treatment in every interventional method. In cases of equivocal findings on morphological imaging procedures, additional functional data can provide information about viable tumor parts. Combined PET/CT imaging systems provide accurate morphological and functional data sets within a single operation^[8].

The aim of this study was to evaluate a potential benefit of combined PET/CT imaging concerning mor-

phology and complementary functional information when assessing the position of an interventional needle within an isolated liver without breathing. This might potentially improve the accuracy of localization of interventional devices compared with morphological imaging alone.

MATERIALS AND METHODS

Lesion model

Ninety artificial lesions, two hypodense, two isodense, and two hyperdense were placed in each of 15 *ex-vivo* pig livers by needle injection. The injected substances consisted of the following ingredients: Hypodense lesions: gelatine (9 g), sodium chloride (NaCl: 20 mL). Isodense lesions: gelatine (9g), NaCl (20 mL), iodine-based contrast agent (0.2 mL/300 mg/mL Xenetix 300, Guerbet GmbH, Sulzbach, Germany). Hyperdense lesions: gelatine (9 g), NaCl (20 mL), iodine-based contrast agent (0.4 mL/300 mg/mL). Additionally 0.5 MBq ^{18}F in form of [^{18}F]-2-Fluoro-2-deoxy-D-glucose (FDG) were administered to all mixtures, thus 0.5 MBq FDG, 20 mL sodium chloride, 9 g of gelatine and the different amounts of contrast agents were used per lesion.

The concentration of FDG was chosen based on previous measurements of differences between tumor and liver background in 75 patients with liver malignancies. A ratio using the differences of Standard Uptake Values (SUV) between the tumor and the liver background was established. Based on this ratio, the amount of FDG was chosen to establish the same ratio between the artificial lesions and the liver background. Seventy-five consecutive patients with metastases of colorectal carcinoma, 25 patients with metastases of NSCLC (non small cell lung cancer) and 10 patients with hepatocellular carcinomas (HCC) were chosen from the local PACS. Patients with HCC were only partly PET-positive tumors or had only low values (SUV), but were chosen to define a broad spectrum of liver malignancies.

Lesion injection and interventional procedure

First, the artificial lesions were injected into the liver with a 7-gauge needle (Figure 1). After injection of the artificial lesion into the *ex-vivo* pig livers, the gelatine mixture hardened as it cooled. Lesion injection and the subsequent interventional device placement were carried out by different physicians. Thus, one physician injected the artificial lesions, while another physician inserted the biopsy needles in the following step.

Second, 18 gauge biopsy needles were inserted (by the second physician) in each liver, one needle in each lesion for a total of 6 needles per *ex-vivo* liver under strict CT-guidance. The needles were only inserted in lesions with favourable shape (round, oval or elliptic) to guarantee reproducible measurements. Lesions which partly dropped away through bile ducts and veins were excluded from the measurements. Additionally, before needle placement, each liver was covered by a thin, non-transparent sheet before needle placement to hide the injection sites.

CT and PET/CT imaging

CT and PET/CT imaging were performed with a Biograph™ system (Siemens Medical Solutions, Hoffman Estates, IL).

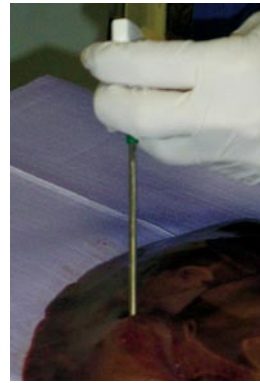


Figure 1 A 7-gauge biopsy needle and a syringe were used for insertion of the gelatine/FDG mixture into the liver. The mixture hardened as it cooled in the *ex-vivo*-liver.

The system consists of two components: a dual-slice CT scanner (Somatom Emotion, Siemens Medical Solutions, Erlangen, Germany) with a minimum gantry rotation time of 800 ms and a full ring PET tomograph (ECAT HR+, Siemens Medical Solutions, Hoffman Estates, IL). The PET system has an axial field of view of 15.5 cm per bed position and an in-plane spatial resolution of 4.6 mm. CT and PET images were acquired consecutively. Repetitive CT scans were carried out for needle positioning with a field-of-view focused on the interventional region. Acquisition parameters for the interventional CT were 120 mAs, 130 kV, 1 mm slice thickness and 1.5 mm table feed.

Following needle placement under strict CT guidance (without using any PET information) a combined PET/CT study was conducted with all needles in position covering the whole *ex-vivo* liver (CT: 120 mAs, 130 kV, 1 mm slice thickness with a 0.5 incremental reconstruction, 1.5 mm table feed, 1 mm collimation, PET: scan time 4 min, 3D data acquisition). CT and PET data sets from the combined imaging approach can be viewed separately or in fused mode on a commercially available computer workstation, which also allows distance measurements on fused images in all three dimensions. Thus, CT images and combined PET/CT images were evaluated separately while all needles inserted within the artificial lesions.

Image evaluation

CT images, either viewed alone or in fused mode (PET/CT), were adjusted to the soft tissue window (center: 50 Hounsfield Units (HU), width: 350 HU). PET images were adjusted to Full Width at Half Maximum (FWHM).

The lesions' width and height were measured in the coronal plane on the commercially available computer workstation and the length was measured in the same way using MPR (multi planar reformatting) in the sagittal direction. The accuracy of CT data alone and combined PET/CT data for determining the needles' position was assessed by measuring the distance (in the horizontal direction) of the needle tip to the lesions' margins on both imaging procedures (CT alone and combined PET/CT) with an electronic calliper in the coronal, transverse and sagittal planes. Imaging measurements from the workstation were correlated with macroscopic measurements after liver lesion dissection, which served as the standard of reference. For this purpose, the liver, with all needles still in place, was finely sliced to measure the distance from the needles' tip to the lesion's margins macroscopically.

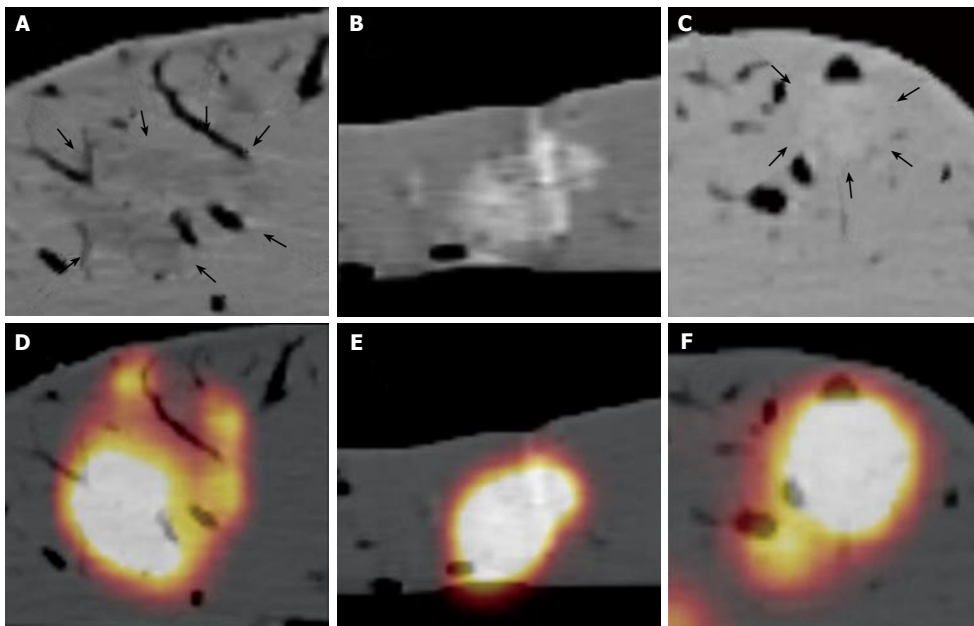


Figure 2 A: This shows a hypodense lesion. The margins of the hypodense lesion are barely seen (fine black arrows). In comparison, the combined PET/CT image of the same lesion shows exactly the margins of the lesion (Figure 2D). Furthermore, the combined PET/CT suggests a different location and extent of the lesion, which was confirmed by the standard of reference. B: This shows a hyperdense lesion. The margins of the lesions are well seen. The combined PET/CT shows the same location and extent of the lesion within the liver tissue (Figure 2E). Thus, in hyperdense lesions, a high correlation of CT and combined PET/CT measurements was found. C: This shows a nearly isodense lesion. The margins of the lesions can only be anticipated (fine black arrows). The corresponding PET/CT (Figure 2 F) of the same lesion shows a different extent of the same lesion with well defined and sharp margins.

All measurements concerning the position of the needle within a single lesion (distances to lesion margin) were compared separately, and the root mean square (RMS) was calculated. The RMS was chosen as a standard description to compare the mean values of different group measurements. The Root Mean Square is calculated as follows:

$$RMS = \sqrt{(x-x_0)^2 + (y-y_0)^2 + (z-z_0)^2}$$

In this formula, x, y and z are defined as the values derived from the macroscopic measurements, serving as the gold standard. In comparison, x₀, y₀ and z₀ are the values from CT measurement or PET/CT measurement. Therefore, in this formula, the values of the gold standard and the values of CT and PET/CT are already compared by calculating the deviation of measurements from CT or PET/CT compared with the macroscopic standard of reference. Thus, greater deviations (meaning less exact definition of the needles' tip on CT or combined PET/CT compared to the standard of reference) will be represented by higher RMS values. In comparison, lower RMS values are calculated based on less deviation of the needles' tip compared to the standard of reference. Values (mean values) were calculated for every lesion based on CT and PET/CT measurements.

Additionally, Hounsfield Units (HU) of every lesion and their surrounding liver tissue was measured and mean values for surrounding tissue and every lesion type were calculated to compare the lesions densities in relation to the liver background. Wilcoxon test for comparing two paired groups was used for statistical analysis.

RESULTS

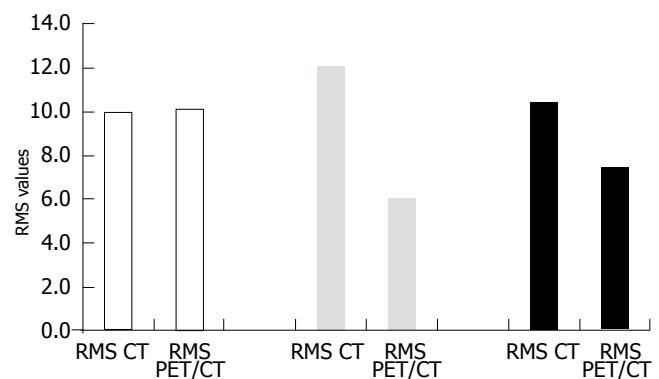


Figure 3 This shows the different mean RMS values for hyper-, iso-, and hypodense lesions. A statistically significant difference was found between the mean RMS values in CT and PET/CT in isodense lesions ($P < 0.05$, grey bars). Additionally, a statistically significant difference was found between the mean RMS values of CT and PET/CT in hypodense lesions ($P < 0.05$, black bars). No difference was found in hyperdense lesions (white bars).

In 90 lesions placed in 15 ex-vivo pig livers, 77 were left in favourable shape for needle intervention (Figure 2). Since several lesions dropped away through bile ducts and veins, 23 hyperdense, 28 isodense, and 26 hypodense lesions were left for measurement.

The mean width was 20.2 (standard deviation (SD): 9 mm) mm, length and height of these lesions were 18.6 (SD: 6 mm) mm, and 16 (SD: 5 mm) mm, respectively, according to the macroscopic standard of reference. Two isodense lesions were missed based on CT data due to poor visibility on the CT images only, whereas both lesions were clearly seen on combined PET/CT images only. The lesions were confirmed by liver dissection. There were no failed punctures in hypo- and hyperdense lesions. The mean RMS for the CT measurements and the combined

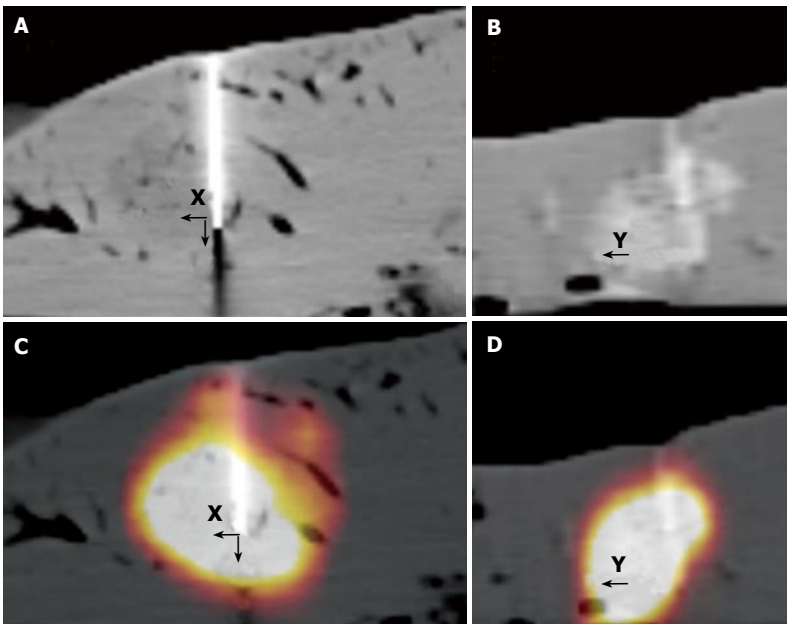


Figure 4 It shows the measurements on the commercially available computer workstation for CT alone (A/B) and combined PET/CT (C/D). The lesions' width and height was measured in coronal direction (Figure 4A and C, X/Z), the lesions' length in sagittal direction (black arrow (Y) in Figure 4 B and D).

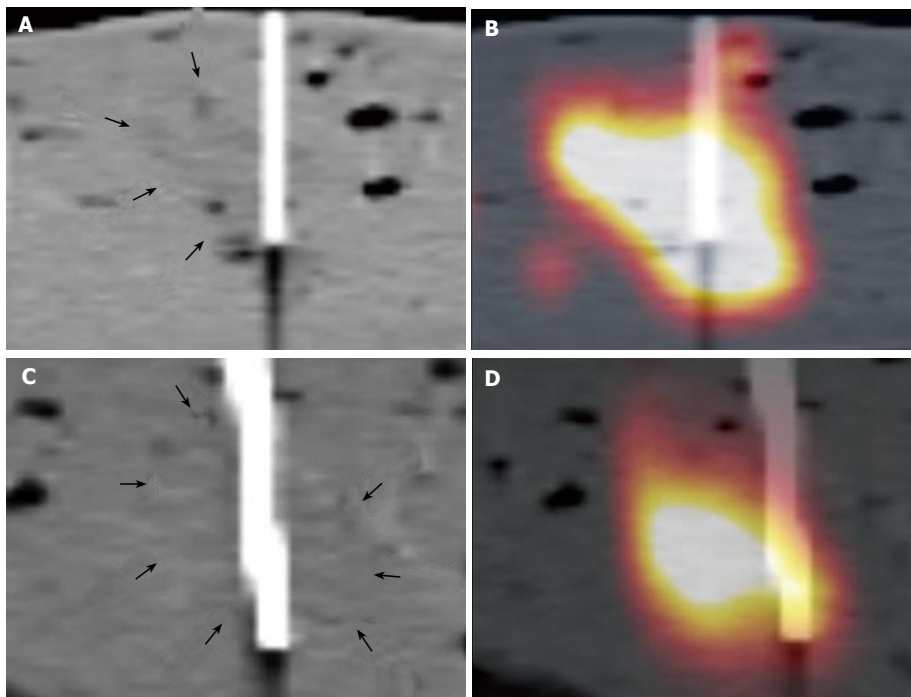


Figure 5 It shows an example of two isodense lesions on CT alone and combined PET/CT with the inserted biopsy needles. The lesions margins are barely seen on CT images alone (fine black arrows, A and C). In comparison, the true extent and localisation of the lesion are well shown on the combined PET/CT images. Based on poor visibility on CT alone, the lesion in the bottom row was nearly missed (D).

PET/CT in hyperdense lesions showed nearly identical values (mean RMS for CT: 10, mean RMS for PET/CT: 10.1) (Figure 3). On the other hand, significant differences were found for the comparison of isodense lesions (mean RMS for CT: 12.1, mean RMS for PET/CT: 6.1). The values for hypodense lesions were less different, however, a significant difference was found here as well (mean RMS for CT: 10.4, mean RMS for PET/CT: 7.4) (Figure 3). Differences between CT and PET/CT were statistically significant in hypodense and isodense lesions ($P < 0.05$ for hypo-, and isodense lesions). Thus, the definition of the needles' position within the lesion on combined PET/CT images was significantly more accurately defined than on CT images alone in hypodense and isodense lesions (Figure 4 and Figure 5). No statistically significant difference between CT-based and PET/CT-based measurements in

hyperdense lesions was found. The distribution of mean Hounsfield Units (HU) for hypodense lesions, isodense lesions and hyperdense lesions, as well as for the surrounding liver tissue with corresponding standard deviation was measured and calculated as well (Figure 6).

The difference between mean values for hypodense lesions compared to the liver background was less than the difference of mean values of hyperdense lesions compared to liver background. Mean values of isodense lesions were only slightly different compared to mean values of the liver background, thus the model of artificial lesions met the requirements of the study.

DISCUSSION

PET/CT imaging proved more accurate when assessing

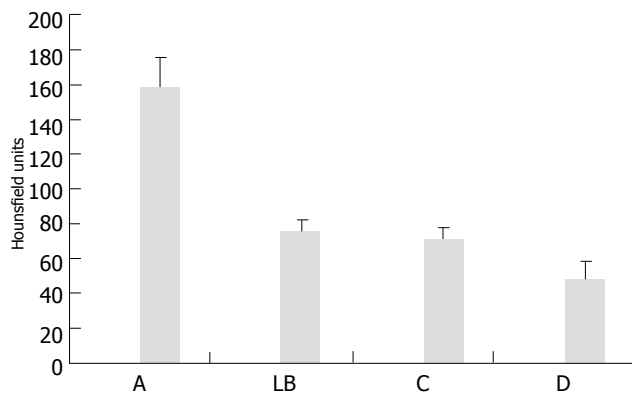


Figure 6 This shows the mean Hounsfield Units (HU) of all measured lesion types, the compared liver background and the corresponding standard deviation. **A:** hyperdense lesions; **LB:** liver background; **C:** isodense lesions; **D:** hypodense lesions.

the position of an interventional device within a liver lesion than imaging analysis based on morphological data alone. Hence, based on the option of more accurate detection of viable tumor tissue, PET/CT promises to add substantial information in selected liver interventions in which equivocal findings on morphologic imaging procedures complicate accurate determination of the interventional needle within the tumour.

Exact positioning of different interventional devices is indispensable for appropriate results in different interventional procedures. In cases of radiofrequency ablation (RFA), complete tumor necrosis is required, because inaccurate position of the ablation device will lead to much higher recurrence rate^[9-11]. In biopsy procedures, however, differentiation of viable tumor tissue and necrosis might sometimes be difficult based on only slight differences in density. Furthermore, exact positioning may sometimes be problematic due to unfavourable shape, size, position and visibility of the lesions.

Although CT is a widely used tool for guidance of interventional procedures^[12-14], even contrast-enhanced CT images may sometimes not be able to distinguish, both the margin of the lesion and the necrotic region from viable tumor fractions. Lesion attenuation values may differ after i.v. contrast enhancement depending on the tumour entity. Thus, metastases of colorectal cancer appear as hypodense lesions within a contrast enhanced liver, whereas HCC as a contrast-enhancing lesion appears with a higher attenuation than the surrounding liver tissue in the arterial phase. However, some lesions may not show lesion to background contrast after i.v. contrast enhancement, they appear isodense. Therefore a lesion model with different densities, representing several contrast enhancing patterns was chosen.

PET/CT provides additional data by adding functional information to morphology and may be of benefit in cases with impaired visibility and only partly viable lesions^[15, 16]. In our study, the needles' positions were significantly better determined on combined PET/CT data sets in hypodense and isodense lesions than with CT alone. Two advantages may arise from these methods from the clinical point of view: first, the placement of the needle

may be performed more accurately in cases with impaired visibility. Although PET/CT puncture itself was not performed in this study, these results are suggesting that the use of the additional functional information can possibly lead to the correct position of the ablative device within the lesion. Thus complete tumour ablation in RFA can be achieved. Second, the assessment of the positioning of interventional devices may be more accurate as well.

Needle positioning was significantly more accurate in hypodense and isodense lesion. While this result may be expected for isodense lesions, it seems rather surprising for hypodense lesions. After all, the needle position in hyperdense lesions was assessed equally well with CT alone and combined PET/CT. These results may be explained by attenuation values of the different lesions types. Differences between attenuation values of hypodense lesions and liver background were less than the difference between the mean Hounsfield Units of hyperdense lesions and liver background. Thus, lesion to background contrast was substantially higher for hyperdense lesions than for hypodense lesions (Figure 6). A further decrease in CT attenuation of hypodense lesions may lead to similar results as detected for hyperdense lesions in this study.

Additionally, two isodense lesions were missed by needle placement based on CT images alone. Primary puncture based on PET/CT images might presumably bring an advantage in visibility and might lead to a successful puncture in these cases.

The study has different limitations. Since it was conducted as an *ex-vivo* trial, patient-induced organ movement was excluded and unfavourable tumor sites close to the diaphragm or the liver hilum could be disregarded. Furthermore, this *ex-vivo* model did not include any background activity which may lead to an increased lesion detectability when assessing the needles' position on combined PET/CT. However, the concentration of FDG injected was chosen based on the described ratio calculated on measurements in patients with different liver malignancies. Thus, we tried to come close to a lesion to background ratio similar to those of patients with a broad average of liver malignancies.

Clinical disadvantages are the small size of the evaluated lesions less than 4 cm in diameter. However, small lesions are the ones most difficult to place an ablative device in. Thus, these are the ones in which CT or other morphological imaging procedures may fail. In addition, interventional procedures with a curative intent are limited to smaller lesions. For example, in RF-ablation the maximal diameter that may successfully be treated is 5 cm. Therefore, the lesion size chosen here met the requirements to simulate clinically often difficult procedures.

Additionally, effective treatment (especially in RFA) can particularly be delivered only to lesions with an appropriate, more or less round, shape. However, primary liver tumors for example can grow beside vessels and bile ducts. In these cases, other therapeutic options have to be considered. Since several lesions in our study setting drained away through bile ducts or veins, these unfavourable lesions were excluded from the evaluation as well.

A general consideration when implementing PET/CT-guided interventions in clinical practice will be its com-

plexity and additional cost compared to CT-guided liver interventions. This approach will be more time-consuming, based on patient preparation with FDG administration one hour prior to the intervention and a substantially longer scan time based on the PET component. Hence, this approach should be limited to cases in which CT alone is not able to accurately assess lesion size, shape and location. A possible clinical procedure when evaluating patients for (diagnostic or therapeutic) interventions could be to conduct a contrast enhanced CT scan first. If the target is well visualized and the lesions' margins are clearly defined on non-enhanced or contrast-enhanced images, a conventional CT-guided intervention might be performed. If the lesion is not clearly defined (hypodense or isodense), a separate PET/CT might be performed to identify the exact localisation and margins of the lesions. The combined PET/CT image then can possibly serve as a landmark tool for the CT-guided intervention. Another step further can be the direct, PET/CT-guided intervention. In this case, the interventional procedure has to be performed directly within the PET/CT system. However, the PET component will require, compared to CT alone, significantly more time, which presumably will be one limiting factor in this scenario. To date, there is no software available where the needle's position can be defined online under combined PET/CT-guidance. Hence, further studies with new technologies have to address the feasibility of this approach. In our opinion, this should be furthermore chosen with focus on cases in which a curative approach is aspired, based on the additional complexity, duration and costs of this procedure.

We conclude that combined PET/CT adds substantial additional information to CT alone when assessing the position of an interventional device within a liver lesion. Thus, co-registered PET/CT can be recommended to date for planning selected liver interventions but, based on its additional complexity and cost, should be limited to those procedures where CT alone is not able to accurately delineate the lesion in question.

ACKNOWLEDGMENTS

The authors thank Thomas Zadow-Eulerich, MD for his intellectual input on this study.

REFERENCES

- 1 **Ballantyne GH**, Quin J. Surgical treatment of liver metastases in patients with colorectal cancer. *Cancer* 1993; **71**: 4252-4266
- 2 **Dromain C**, de Baere T, Elias D, Kuoch V, Ducreux M, Boige V, Petrow P, Roche A, Sigal R. Hepatic tumors treated with percutaneous radio-frequency ablation: CT and MR imaging follow-up. *Radiology* 2002; **223**: 255-262
- 3 **Nahum Goldberg S**, Dupuy DE. Image-guided radiofrequency tumor ablation: challenges and opportunities--part I. *J Vasc Interv Radiol* 2001; **12**: 1021-1032
- 4 **Dupuy DE**, Goldberg SN. Image-guided radiofrequency tumor ablation: challenges and opportunities--part II. *J Vasc Interv Radiol* 2001; **12**: 1135-1148
- 5 **Wood TF**, Rose DM, Chung M, Allegra DP, Foshag LJ, Bilchik AJ. Radiofrequency ablation of 231 unresectable hepatic tumors: indications, limitations, and complications. *Ann Surg Oncol* 2000; **7**: 593-600
- 6 **Stewart CJ**, Coldewey J, Stewart IS. Comparison of fine needle aspiration cytology and needle core biopsy in the diagnosis of radiologically detected abdominal lesions. *J Clin Pathol* 2002; **55**: 93-97
- 7 **Yu SC**, Liew CT, Lau WY, Leung TW, Metreweli C. US-guided percutaneous biopsy of small (<or = 1-cm) hepatic lesions. *Radiology* 2001; **218**: 195-199
- 8 **Beyer T**, Townsend DW, Brun T, Kinahan PE, Charron M, Roddy R, Jerin J, Young J, Byars L, Nutt R. A combined PET/CT scanner for clinical oncology. *J Nucl Med* 2000; **41**: 1369-1379
- 9 **Goldberg SN**, Gazelle GS, Mueller PR. Thermal ablation therapy for focal malignancy: a unified approach to underlying principles, techniques, and diagnostic imaging guidance. *AJR Am J Roentgenol* 2000; **174**: 323-331
- 10 **Rossi S**, Di Stasi M, Buscarini E, Quaretti P, Garbagnati F, Squassante L, Paties CT, Silverman DE, Buscarini L. Percutaneous RF interstitial thermal ablation in the treatment of hepatic cancer. *AJR Am J Roentgenol* 1996; **167**: 759-768
- 11 **de Baere T**, Elias D, Dromain C, Din MG, Kuoch V, Ducreux M, Boige V, Lassau N, Marteau V, Lasser P, Roche A. Radiofrequency ablation of 100 hepatic metastases with a mean follow-up of more than 1 year. *AJR Am J Roentgenol* 2000; **175**: 1619-1625
- 12 **Schmidt AJ**, Kee ST, Sze DY, Daniel BL, Razavi MK, Semba CP, Dake MD. Diagnostic yield of MR-guided liver biopsies compared with CT- and US-guided liver biopsies. *J Vasc Interv Radiol* 1999; **10**: 1323-1329
- 13 **Welch TJ**, Sheedy PF 2nd, Johnson CD, Johnson CM, Stephens DH. CT-guided biopsy: prospective analysis of 1,000 procedures. *Radiology* 1989; **171**: 493-496
- 14 **Antoch G**, Kuehl H, Vogt FM, Debatin JF, Stattaus J. Value of CT volume imaging for optimal placement of radiofrequency ablation probes in liver lesions. *J Vasc Interv Radiol* 2002; **13**: 1155-1161
- 15 **Antoch G**, Stattaus J, Nemat AT, Marnitz S, Beyer T, Kuehl H, Bockisch A, Debatin JF, Freudenberg LS. Non-small cell lung cancer: dual-modality PET/CT in preoperative staging. *Radiology* 2003; **229**: 526-533
- 16 **Antoch G**, Vogt FM, Freudenberg LS, Nazaradeh F, Goehde SC, Barkhausen J, Dahmen G, Bockisch A, Debatin JF, Ruehm SG. Whole-body dual-modality PET/CT and whole-body MRI for tumor staging in oncology. *JAMA* 2003; **290**: 3199-3206

S- Editor Wang J L- Editor Pravda J E- Editor Zhang Y